

Highly blue emission of ZnO nanoparticles embedded in a SiO₂ matrix

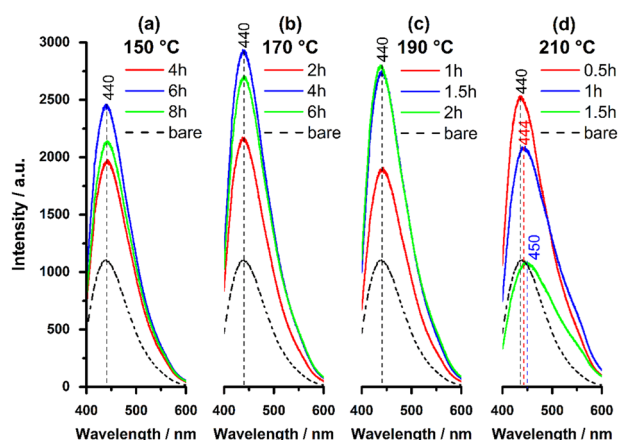
Joan Reyes Miranda¹ · Felipe de Jesús Carrillo Romo¹ · Antonieta García Murillo¹ · Ángel de Jesús Morales Ramírez¹ · A. Garrido Hernández²

Received: 30 November 2016 / Accepted: 9 March 2017 / Published online: 3 April 2017
© Springer Science+Business Media New York 2017

Abstract The main drawbacks of fluorescent ZnO nanoparticles in practical optoelectronic applications are fast particle growth and agglomeration in water, causing a periodic decrease of light emission intensity. In this work, ZnO nanoparticles were successfully embedded within a silica matrix to prevent their agglomeration. The ZnO NPs were synthesized by the polyol method, using ethylene glycol and glycerol in sizes ranging from 5–6 nm. The as-obtained ZnO particles were dispersed in an amorphous silica matrix under three different ZnO:SiO₂ molar ratios: 20:80, 15:85 and 10:90. With the aim of enhancing the luminescent properties of the ZnO@SiO₂ composites, various annealing treatments in the range of 150–210 °C were carried out. The chemical analyses of the bare ZnO and the composites were carried out by Fourier transform infrared spectroscopy, which confirmed the presence of functional groups attached to the ZnO surface. By means of thermogravimetric analysis, it was determined that the evaporation of solvents shifted to lower temperatures (180 °C) when silica was added to the ZnO colloidal solution. By means of photoluminescence, a bright blue emission, centered at 440 nm, was observed in all of the samples, even at high temperatures (i.e., 210 °C); only a red shift of 20 nm was observed. Interestingly, the emission intensity of the sample 20:80,

when annealed at 170 °C for 4 h, was enhanced 2.6 times, compared to the bare ZnO.

Graphical Abstract



Keywords Nanoparticles · Composite · Blue emission · Zinc oxide · Silica

1 Introduction

In recent years, fluorescent semiconductor nanoparticles (NPs), free of toxicity, low in cost, and easy to produce, have attracted considerable attention due to their wide range of applications, such as for use in biological labeling [1, 2], light emitting diodes (LEDs) [3, 4], photocatalysis [5, 6], solar cells [7, 8] and so on. This is the case with ZnO, which has a wide band gap (3.37 eV) and high exciton binding

✉ Antonieta García Murillo
angarciam@ipn.mx

¹ Instituto Politécnico Nacional, CIITEC IPN, Cerrada de Cecati S/N. Col. Santa Catarina, Azcapotzalco México D.F. C.P, Mexico, Santa Catarina 02250, Mexico

² Universidad Tecnológica de Tecámac, UTTEC, Carretera Federal México, Pachuca Km 37.5, Col. Sierra Hermosa, Tecámac, Estado de México CP 55740, Mexico

energy (60 meV), resulting in bright room temperature emission.

The visible light emission of ZnO is only exhibit at nanoscale, less than 10 nm [9]; at this scale, the high surface area to volume ratio of nanoparticles promotes the formation of high point defects concentration, such as oxygen vacancies (V_o), zinc vacancies (V_{zn}), oxygen interstitials (O_i), zinc interstitials (Zn_i), and antisite oxygen (O_{zn}), thus, the visible emission from blue to green depends on the energy transition of this points defects [10, 11].

To enhance the potential of ZnO NPs, simple synthesis methods that are able to produce intense light emissions, stability, and reproducible results are required. ZnO NPs are synthesized using several methods in liquid phase; the conventional one is the sol–gel process using LiOH–H₂O and Zn(Ac)₂ in an alcoholic medium [11–16] or a similar process with certain modifications [17, 18]. Another method is the polyol process, consisting of the hydrolysis of zinc salts in a polyol medium—ethylene glycol (EG), diethylene glycol, triethylene glycol (TG), or glycerol (GLY) [19–22]. The use of polyols for the synthesis of NPs provides a variety of advantages; they make it possible to obtain colloidal stable suspensions of non-agglomerated particles, a narrow size distribution, high crystallinity, and controlled morphology [19].

However, the main drawback of ZnO NPs in practical optoelectronic applications is their poor stability in aqueous environments and low temperatures (50–80 °C); the hydroxyl groups attack and easily destroy the luminescent centers (point defects) on the ZnO surface, causing agglomeration and promoting particle growth which provokes periodic decreases in light emission intensity.

Great efforts have been made to protect the surfaces of ZnO NPs. Adding a protective SiO₂ shell around NPs ZnO is an excellent approach for increasing stability and halting the growth process. The protective shell is normally deposited on the ZnO NPs surface by hydrolysis and condensation reaction of tetraethyl orthosilicate (TEOS) in an alcoholic medium, then the product obtained is isolated by centrifugation and re-dispersed in an aqueous medium [13, 14, 23–26]. In this regard, Wang et. al., [13] demonstrated the stability of ZnO NPs@SiO₂ for up to 4 months when dispersed in water, while bare ZnO NPs dispersed in water started to aggregate and finally produce precipitates from the dispersion even after 10 min; moreover, a red shift emission and quenched luminescent properties have been observed in bare ZnO NPs. The emission intensity of ZnO@SiO₂ was observed to be comparable to freshly bare ZnO NPs. Hagura et. al. [14] also demonstrated the stability of silica-coated ZnO NPs in water, but the composite was synthesized at different temperatures (50–75 °C). The PL results show that heating was necessary to obtain visible emissions, finding that as temperature increases, the

emission intensity increases too, up to 70 °C, and then declined. Thus, thin silica shells are feasible only at low temperatures (i.e., 70 °C), where particle growth and red shift are accompanied by quenched optical properties.

In the previous cited reports, no mention is made of the effect that a high silica concentration has on luminescent properties. In our previous work [27], we successfully embedded BaTiO₃:Eu³⁺ particles in a SiO₂ matrix and found that the luminescent emission intensity increased as the silica concentration increased, up to a Ba:Si molar ratio equal to 5:95; this approach using a high SiO₂ concentration also increased the amount of luminescent material, making it considerably cheaper than bare luminescent particles.

In this instance, ZnO NPs were confined in a high SiO₂ concentration (80–95 molar%), which resulted in greatly enhanced blue emission. The ZnO NPs were prepared by polyol method in EG and GLY as solvents. Then, the colloidal ZnO NPs were mixed by ultrasound with the TEOS solution. The powders obtained after dried at 100 °C were thermally annealed at temperatures ranging from 150 to 210 °C for various lengths of time. We demonstrated that a high SiO₂ concentration retards ZnO particle growth, even at temperatures of 210 °C, and no considerable red shift was observed, maintaining the blue emission from all of the samples.

2 Experimental details

2.1 Synthesis of ZnO NPs

Zinc acetate dehydrate (Zn(CH₃COO)₂ · 2H₂O); Sigma Aldrich, 98%), EG (C₂H₆O₂; Fermont, 99.8%), GLY (C₃H₈O₃; Sigma-Aldrich) and chlorhydric acid (HCl, Fermont 37.1%) were used without further purification. For a typical polyol synthesis, 4.5 mmol of Zn(Ac)₂ · 2H₂O were dissolved in 7.5 ml of ethylene glycol under vigorous stirring for 10 min; afterwards, 7.5 ml of glycerol and 2.25 ml H₂O were added to the solution. Then the mixture was heated at 90 °C. Immediately, the solution turned brown, indicating that ZnO NPs were beginning to nucleate and grow. After 30 min, NPs started to precipitate, and 1 mL of HCl was added to prevent precipitation. Finally, the colloidal solution was maintained at the same temperature for 5 h in order to evaporate the solvents, and 4 ml of colloidal solution was obtained. The ZnO NPs had a hydrophilic character, yielding a very stable solution in water, without losing their luminescent properties.

2.2 Sol–gel synthesis of SiO₂

The precursors used to synthesize the silica matrix by the sol–gel method were tetraethyl orthosilicate ((Si(OC₂H₅)₄,

98%, TEOS), ethanol ($\text{CH}_3\text{CH}_2\text{OH}$, 99.9% Fermont), hydrochloric acid (HCl 37.1 %, Fermont), and distilled water. The procedure was the same as that reported in previous work [27]. In short, 22.39 mmol of TEOS was dissolved in ethanol; a solution of ethanol/TEOS with a molar ratio of 4:1 was prepared according to Klein's diagram [28]. Afterwards, 3 ml of hydrochloric acid (1 M) aqueous solution was prepared and kept stirring for 1 h. Finally, this last solution was added to the ethanol/TEOS solution and kept stirring for 21 h.

2.3 Synthesis of ZnO NPs@SiO₂ composites

In order to prepare ZnO NPs@SiO₂ systems, 1.125 mmol (1 ml) of ZnO NPs colloidal solution was mixed by ultrasound with an appropriate volume of the synthesized SiO₂ sol. Three different ZnO-NPs/SiO₂ molar ratios: 20:80, 15:85 and 10:90—were synthesized. In addition, a pure sample of ZnO was considered. The ZnO NPs colloidal solution was completely dissolved in the SiO₂ sol, forming a transparent and uniform solution. The mixture was dried in an oven at 100 °C for 5 h. Finally, the composites obtained were annealed at 150, 170, 190, and 210 °C for different lengths of time. Table 1 summarizes the synthesis conditions of the composites.

2.4 Characterization

Infrared (IR) measurements were performed on a Perkin Elmer 2000 spectrometer, using the KBr pellet method. For all measurements, the spectra were recorded from 4000 to 400 cm^{-1} . Thermogravimetric analysis (TGA) was carried out using a DTG60 detector in a nitrogen atmosphere, with a heating rate of 5 °C·min⁻¹. High resolution transmission electron micrographs (HRTEM) were obtained on a JEOL

JEM-2100 operating at 200 kV. The samples were ground and dispersed in isopropanol under ultrasonic conditions, and then an aliquot of the prepared solution was dropped on a carbon-coated copper grid. The emission and excitation spectra of the samples were recorded on a F-7000 fluorescence spectrophotometer, using a 450 W xenon lamp. The final uncertainty in the emission and excitation spectra was 16.8 u.a of intensity (y axis) and 0.18 nm of wavelength (on the x axis), with a confidence level of 95%.

3 Results and discussion

3.1 FTIR and TG analyses of ZnO NPs and ZnO:SiO₂ composites

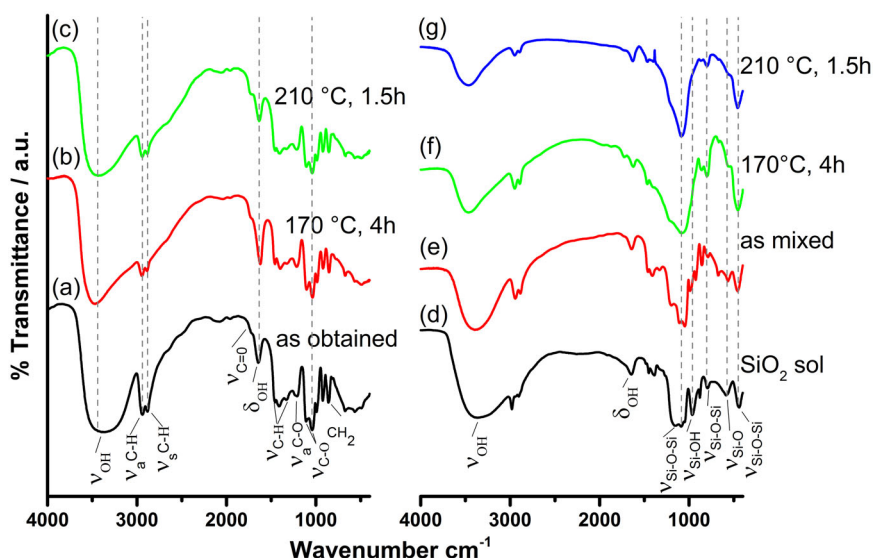
The FTIR spectra of the ZnO NPs and ZnO:SiO₂ composites (sample A), treated at 170 and 210 °C, are depicted in Fig. 1a–c and d–g, respectively. In Fig. 1a–c, functional groups attached to the ZnO particles are detected in the 4000–900 cm^{-1} region. A broad band in the range 3600–3000 cm^{-1} in all of the samples is attributable to the stretching vibrations of hydroxyl groups (νOH), arising from water chemically and physically adsorbed on the ZnO NPs, and the band centered at 1634 cm^{-1} is related to the OH deformation vibrations (δOH) of the absorbed water [29].

The bands centered at 2932 and 2874 cm^{-1} can be attributed to asymmetric and symmetric C–H stretching vibrations. As well, the bands at 1459, 1407, 1327, and 858 cm^{-1} are related to the C–H bending associated with CH₂. The bands at 1085 and 1035 are related to the C–O bond stretching of C–O–C groups ($\nu_{\text{C-O}}$); in addition, a band corresponding to asymmetric C–O–C stretching vibrations is observed at 1220 cm^{-1} , all the as mentioned functional groups are characteristics of GLY and EG spectra [30, 31]

Table 1 Synthesis' parameters of the ZnO NPs /SiO₂ composites

Sample	ZnO NPs (mmol)	SiO ₂ (mmol)	Molar ratio ZnO/SiO ₂	Temperature (°C)	Time (H)
ZnO	1.125	–	100:0	–	–
A	1.125	4.25	20:80	150	4, 6, 8
				170	2, 4, 6
				190	1, 1.5, 2
				210	0.5, 1, 1.5
B	1.125	6.37	15:85	150	4, 6, 8
				170	2, 4, 6
				190	1, 1.5, 2
				210	0.5, 1, 1.5
C	1.125	10.12	10:90	150	4, 6, 8
				170	2, 4, 6
				190	1, 1.5, 2
				210	0.5, 1, 1.5

Fig. 1 a–c FTIR spectra of the ZnO colloidal solution; d–g ZnO@SiO₂ sample 20:80 under different annealing conditions



and remained in the sample after annealed at 170 °C at 210 °C (Fig. 1a–c). The spectra also show the characteristic stretching vibrations of esters C=O at 1729 cm⁻¹ [29], this band is the only one not present in the GLY and EG spectra. Tang et al. [32] related the stability of ZnO nanoparticles in water to a single ester compound attached to the surface. The C–H stretching vibrations at 2932 and 2874 cm⁻¹ and the band assigned to the OH deformation vibrations significantly decreased as temperature increases but not disappeared completely. In addition, no Zn–O vibrations at low ranges were detected; however, considering the transmission electron micrographs, various interplanar distances were indexed to the ZnO wurtzite structure (Section 3.2.).

Fig. 1d shows the IR spectrum of the SiO₂ sol before it was added to the ZnO colloidal solution. The absorption bands centered at 960 cm⁻¹ are associated with silanol groups (SiOH), and the band centered at 585 cm⁻¹ can be assigned to ethoxy groups (Si(OC₂H₅)); both are products of the hydrolysis of TEOS [28]; at the same time, a condensation reaction between SiOH and the ethoxy groups (SiOC₂H₅) was carried out, and siloxane groups (Si–O–Si) were formed, which is reflected at 1080 cm⁻¹ in the symmetry stretching of SiO₄ tetrahedra, at 798 and 450 cm⁻¹ [33]. After the ZnO colloidal solution and the SiO₂ sol (Fig. 1e) were mixed, functional infrared bands characterizing the EG and GLY groups of solvents, and SiO₂ bonding, appeared. However, the silanol and ethoxy bands in Fig. 1f–g were completely removed after 170 and 210 °C thermal annealing, promoting a complete transformation of ethoxy to silanol groups, and then silanol to siloxane groups.

A determination of the effects of silica on thermal properties of ZnO NPs was carried out by TGA. Figure 2 shows the TGA profile of the as-synthesized ZnO NPs. A first weight loss of 10% is seen at 160 °C, which can be associated with water evaporation and initial evaporation of the

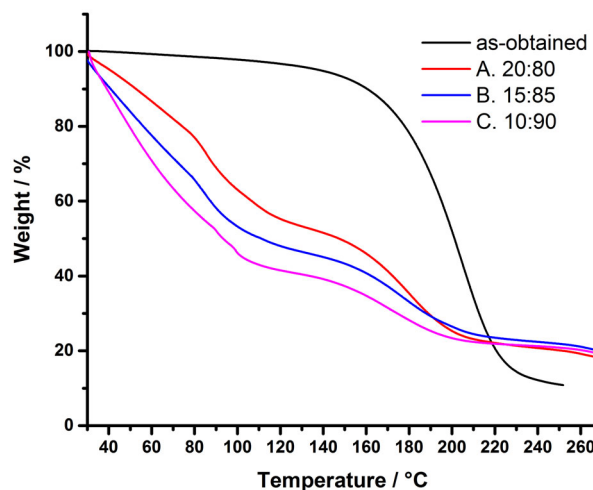
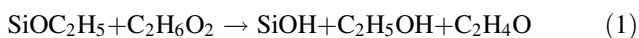


Fig. 2 TGA curves of the as-obtained ZnO NPs and samples a, b, and c

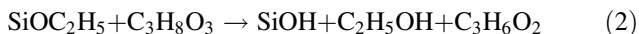
EG. Maximal weight loss occurs in the range of 170–210 °C, due to EG and GLY evaporation. The boiling point of EG is around 195–198 °C, while GLY starts boiling at 182 °C. A maximal weight loss of 89% was recorded at 260 °C.

However, the TGA profile of the composite A (20:80) shows that the weight loss occurred at lower temperatures. Once the ZnO colloidal solution and the SiO₂ sol were mixed, the hydrolysis of the ethoxy groups (SiOC₂H₅) could be carried out by the EG and GLY. Ravaine et al. [34] prepared silicates by mixing TEOS with polyethylene glycol (PEG). From chemical analysis and weight measurement, they determine that the reaction between tetraethoxy groups and PEG produces polyethylene oxide. Ștefănescu et al. [35] studied the interaction among TEOS and different polyols (EG, 1–2 propane diol, 1–3 propane diol, and GLY), they demonstrated the formation of different species

depending on the polyol. In this regard, ethoxy groups can react with EG to form ethylene oxide (C_2H_4O):



while the reaction between the ethoxy groups and glycerol could create glycidol ($C_3H_6O_2$):



The initial boiling points of ethylene oxide and glycidol are around 11 and 62 °C, respectively. This could explain why a weight loss of 10% occurred at 52 °C instead of 160 °C, as was observed with the bare ZnO colloidal solution. Moreover, the greater the silica concentration, the greater the weight loss. For example, at 170 °C, a weight loss of 58.7, 62.8, and 68.5% occurred in samples A, B, and C, respectively. Considering that the volume of the ZnO solution was constant (1 mL) and that the volume of the SiO_2 sol was increasing in samples A (2.5 mL), B (3.6 mL), and C (5.7 mL), it is possible that in sample A, the hydrolysis of the ethoxy groups ($SiOC_2H_5$) was completed with a small concentration of EG and GLY, while for sample C (with the highest concentration of ethoxy groups) most of the EG and GLY molecules reacted, showing a greater weight loss, at 170 °C (Fig. 2).

3.2 Structural and morphological analysis

In order to confirm the formation of ZnO@ SiO_2 composites and study the effects of heat treatment temperatures on particle size and crystallinity, morphological analyses were carried out on sample A (20:80), heat treated at 170 °C for 4 h and 210 °C for 1.5 h (see Fig. 3a–b and d–e, respectively). It can be seen that both samples show quasi-spherical ZnO particles (*black zones*) well confined in the protective silica matrix (*grey*). For the sample annealed at 170 °C, the ZnO particle diameter was around 7–10 nm, but as the temperature increased to 210 °C, the particle size increased slightly, to ~10–13 nm; furthermore, the lattice fringes are more defined (Fig. 3d), indicating a greater crystallinity of the ZnO NPs. Fig. 3c, f show the lattice fringes with interplanar distances of 0.279 and 0.265 nm, determined by Fourier transform and corresponding to the (100) and (002) planes of the hexagonal wurzite structure, as reported by [15, 23, 36].

3.3 Photoluminescence

The luminescent properties of the as-synthesized colloidal solution and the ZnO NPs @ SiO_2 composite powders were evaluated. The luminescent properties of the composites were evaluated as a function of the annealing treatment in the range of 150–210 °C for different lengths of time. Fig. 4 shows the room PL excitation and the emission spectra of

the as-prepared colloidal ZnO NPs. The emission spectrum shows a bright blue emission centered mainly at 440 nm under 357-nm excitation, and no UV emission was recorded in the spectrum; which is observed only in highly crystalline samples [11, 37]. Although the visible emission of ZnO NPs is not completely understood, usually it is related to transitions from point defects such as V_o , V_{zn} , O_i , Zn_i , and O_{zn} [10, 16]. It has been reported that the energy level of Zn_i consists of a shallow donor level located about 0.35 eV below the conduction band, and that it is responsible for the blue emission, such that one electron trapped in the Zn_i and a hole in the V_{zn} can recombine [15, 17, 38]. The inset photograph shows the bright blue emission of the ZnO colloidal solution; it was taken 3 months later of synthesized under a 365 nm UV lamp.

According to the effective mass model developed by Brus [9], the crystallite size can be calculated from the peak wavelength of the excitation spectra by using the Eq. 3.

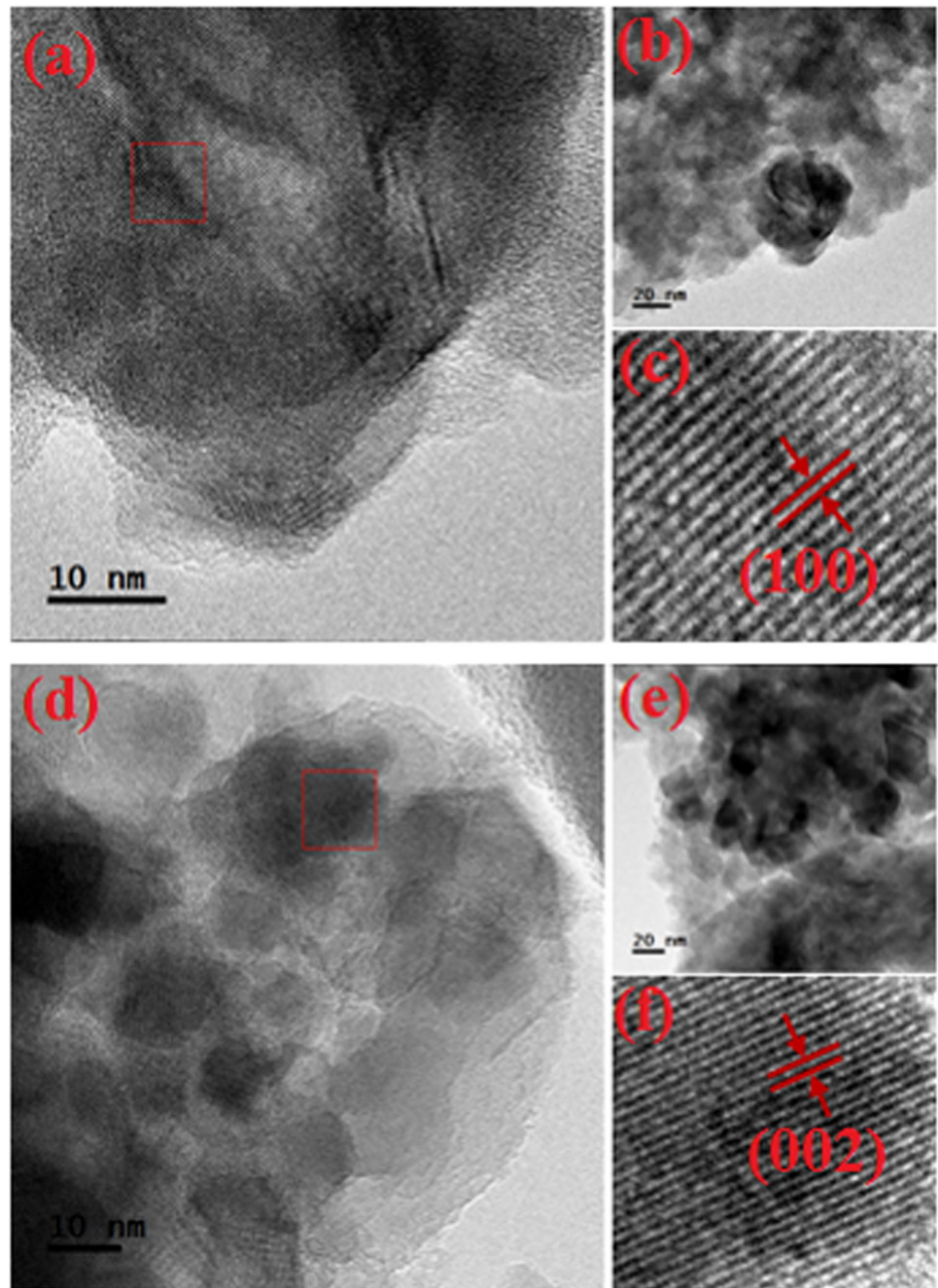
$$E_g^{QDs} = E_g^{bulk} + \frac{h^2}{2D^2} \cdot \left(\frac{1}{m_e^*} + \frac{1}{m_h^*} \right) - \frac{1.8e^2}{2\pi\epsilon_0\epsilon D} \quad (3)$$

where E_g^{bulk} is the bulk bandgap (3.37 eV), h is the Planck constant, ϵ_0 is the permittivity of free space, ϵ is the relative permittivity of ZnO, and $m_e^* = 0.24m_e$ and $m_h^* = 0.45m_e$ are the effective mass of the electrons and the effective mass of the holes, respectively [9, 14]. Based on the excitation spectra (Fig. 4), the calculated crystallite size is around 5–6 nm.

Figure 5 shows the excitation spectra of samples A and C annealed at 170 and 210 °C for 4 h and 1.5 h, respectively, under an emission wavelength of 440 nm. For reference, the excitation spectrum of the ZnO colloidal solution is included. In the graphs, a red shift is observed as the temperature rises from 170 to 210 °C indicating agglomeration and particle growth. This red shift is no larger than 20 nm and 12 nm for samples A and C, respectively. The lower shift in sample C can be attributed to higher silica concentration compared to that in sample A, this assumption is based on the transmission electron microscopy (TEM) images (Fig. 3), where it is observed a non-complete isolation of each ZnO NP into the silica matrix and with the rise of temperature the nearest particles begin to agglomerate, giving place to the particle growing. Besides, with a higher SiO_2 concentration, it is expected a bigger dispersion of the ZnO NPs, therefore their protection against agglomeration and growth particle even at high temperatures (210 °C) is enhanced. Hagura et al. [14] reported a red shift of 14 nm when samples were annealed from 50 to 75 °C, due to a low silica concentration.

With the Brus model, the crystallite sizes of samples A, B, and C were also calculated from their respective excitation spectra. According to the HRTEM images of sample A annealed at 170 °C for 4 h and 210 °C for 1.5 h, the

Fig. 3 TEM images of sample A annealed at 170 °C **a–c** and at 210 °C **d–f**



crystallite size is about 5–7 nm and 10–13 nm, respectively, this sizes values are in agreement with the size calculated by the Brus model with size around 7.3 and 12.1 nm, respectively (Table 2). As expected the ZnO particle growth in samples A, B, and C is bigger when annealed at 210 °C for 1.5 h. Interestingly, the particle growth of sample C (10:90) annealed from 170 to 210 °C is less than 2 nm. Thus, the higher the silica concentration, the higher the protection against agglomeration and growth particle.

In order to find the optimal synthesis conditions for increasing the emission intensity of ZnO-NPs-/SiO₂

composites, the room PL emission spectra of sample A were determined under different annealing treatments, Fig. 6A(a). Like the as-prepared colloidal solution, the composites show a bright blue emission centered mainly at 440 nm; all of the spectra were recorded under 365 nm excitation. It is important to point out that the luminescent properties of composite systems change significantly as a function of temperature. When the sample was annealed at 150 °C for 4, 6, and 8 h, the emission intensity increased by 1.7, 2.2, and 1.9 times, respectively, 6 h being the optimal time for this temperature. This enhancement of the emission

intensity is related to the partial evaporation of the solvents (i.e., EG and GLY), as demonstrated by TGA, with a weight loss of 50–60% at 150 °C (Section 3.1). Because the partial prevention of agglomeration and growth particle, the rich point defects Zn_i and V_{zn} on the surface and their energy levels were not affected; as a consequence, only a blue emission without red shift is observed even at 8 h of annealing. However, for 8 h of annealing, the solvent evaporation and the crystallinity increases, as shown by the transmission electron micrographs (Section 3.2), causing a reduction of point defect concentrations, and thus, the emission intensity is affected.

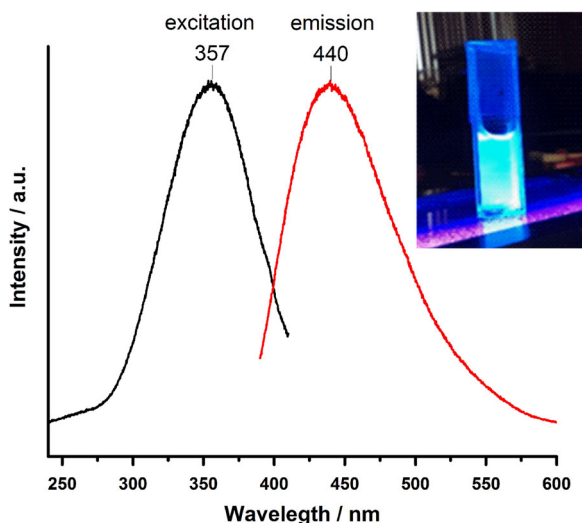
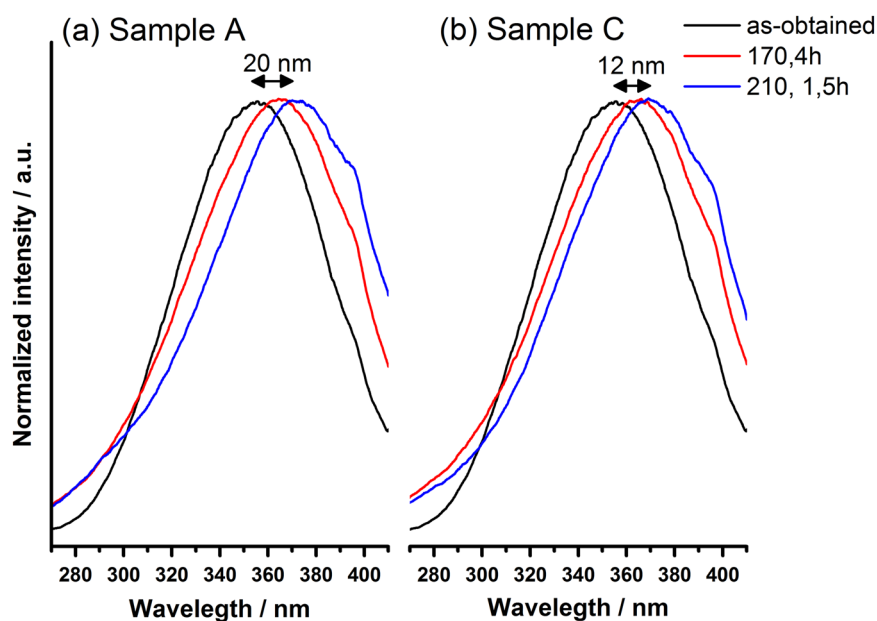


Fig. 4 PL excitation (*left*) and emission spectra (*right*) of the as-synthesized ZnO NPs. Inset: Direct photograph of ZnO NPs under a 365 nm excitation lamp

Fig. 5 Excitation spectra of **a** sample A and **b** sample C annealed at 170 and 210 °C, respectively



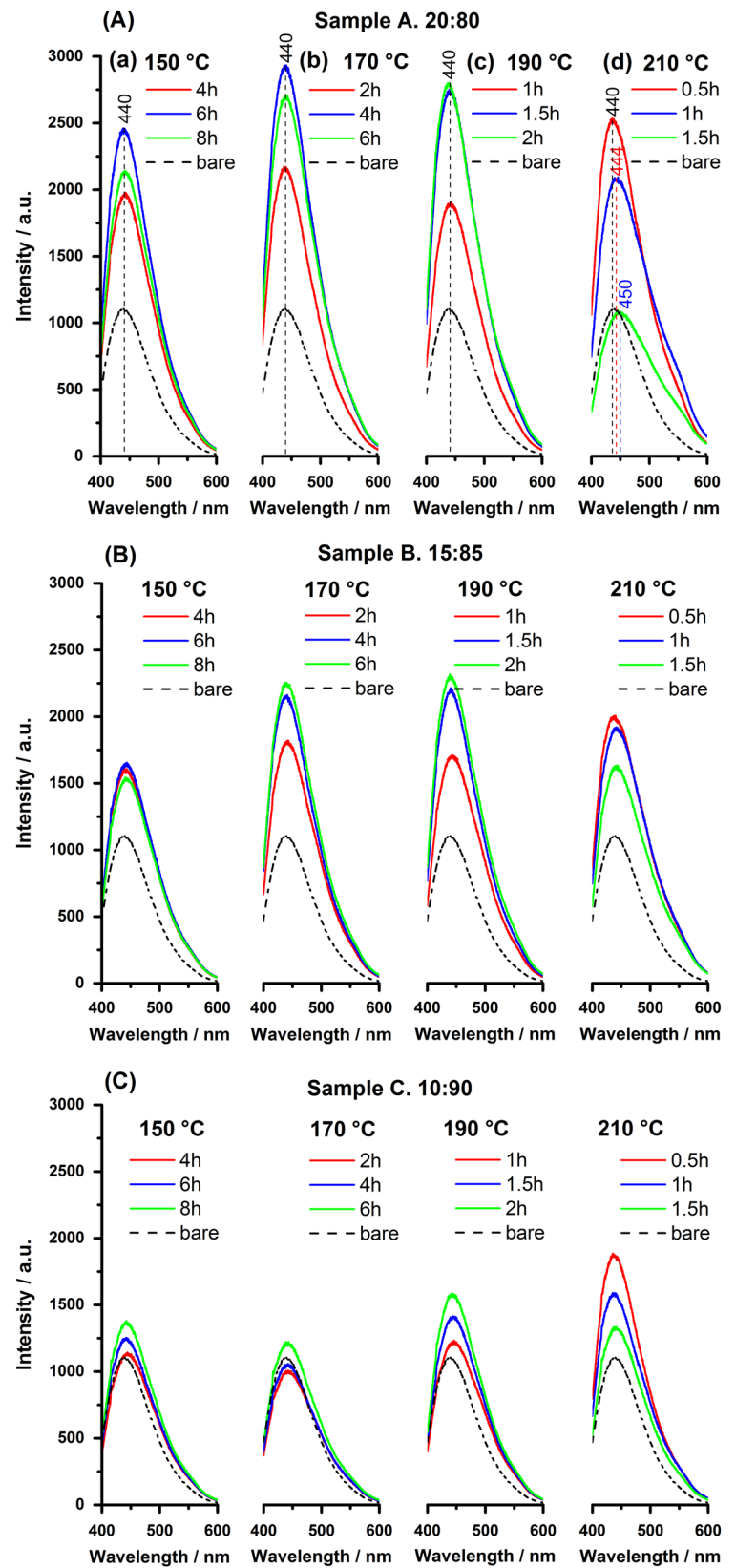
In addition, as the temperature increases from 150 to 170 °C, less time is required for enhancing the blue emission intensity; the emission improvement is 1.9, 2.6, and 2.4 times for 2, 4, and 6 h, respectively, as observed in Fig. 6A (b). Only 20 °C more significantly reduces the time required. This behavior is related to faster solvent evaporation than occurred at 150 °C, which also is evident upon observing the TG analyses. Moreover, the boiling point of TEOS is around 168 °C; therefore, full polymerization of TEOS may have occurred at this temperature. These conditions were established as optimal for enhancing the emission intensity of the composite systems.

Fig. 6A(c) shows the emission spectra of the composite annealed at 190 °C. The emission for a treatment lasting 2 h is similar to those for a 4-h treatment at 170 °C; these 20 °C difference reduced the time to 2 h. Finally, the sample annealed at 210 °C for 0.5 h yielded the highest intensity at this temperature (Fig. 6A(d)), then an abrupt reduction was observed as the time increased to 1.5 h. Under these

Table 2 Crystallite size of the composite powders under different annealing conditions according to the Brus model

Annealing conditions	Sample A 20:80	Sample B 15:85	Sample C 10:90
	Crystallite size/nm		
170 °C, 2 h	6.95 ± 0.05	6.39 ± 0.04	6.17 ± 0.02
170 °C, 4 h	7.32 ± 0.06	6.39 ± 0.04	6.17 ± 0.02
170 °C, 6 h	7.77 ± 0.08	6.65 ± 0.05	6.39 ± 0.04
210 °C, 0.5 h	9.50 ± 0.2	9.30 ± 0.15	6.95 ± 0.05
210 °C, 1 h	11.28 ± 0.63	9.30 ± 0.15	7.32 ± 0.06
210 °C, 1.5 h	12.14 ± 1.2	10.25 ± 0.3	7.79 ± 0.08

Fig. 6 PL emission spectra of the ZnO@SiO₂ composites. **a** sample A, **b** sample B, and **c** sample C. All of them under different annealing treatments



annealing conditions, the particle size calculated was about 12.14 nm (Table 2) and according to Brus [9] the luminescent properties of ZnO NPs are increased as the particle size decreased from 10 nm due to the higher surface to volume ratio that promotes the formation of higher point defects concentration, therefore, a lower concentration of point defects (Zn_i and V_{zn}) on the surface promotes a reduction in the emission intensity. It is worth mentioning that even under these extreme conditions (210 °C, 1.5 h.), a red shift no greater than 10 nm was observed.

On the other hand, although the bare ZnO-NPs (*dashed curve*) and the composite treated at 210 °C for 1.5 h (*green*

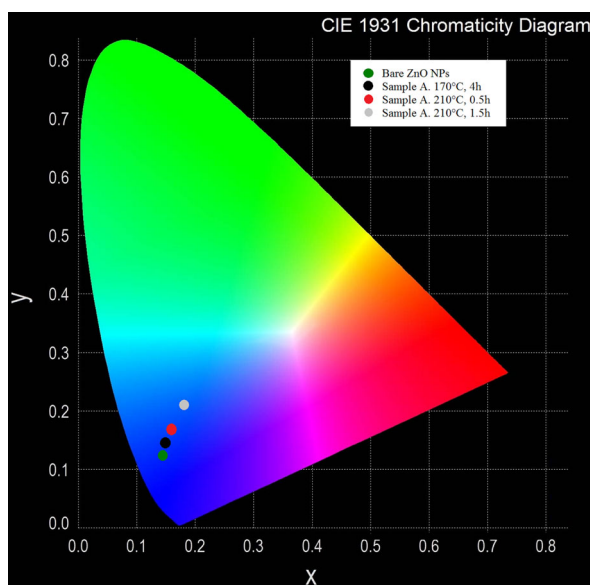
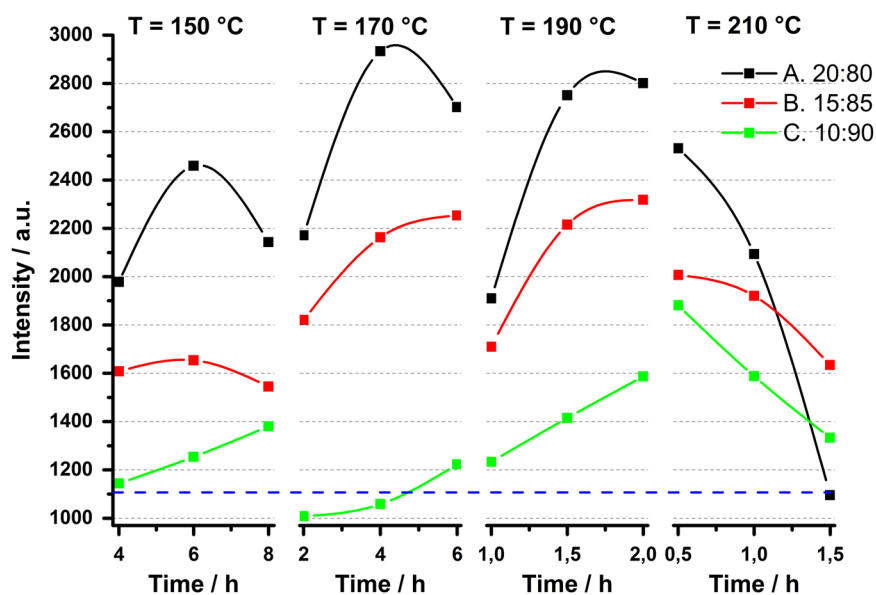


Fig. 7 CIE coordinates of the bare ZnO solution and sample A annealed at 170 and 210 °C

Fig. 8 Maximal emission intensities of samples a, b, and c at a temperature range of 150–210 °C



curve) in Fig. 6A(d) have similar emission intensities, the latter shows a broad emission, and, therefore, the emitted color can be expected to be different. Figure 7 shows the CIE coordinates for the bare ZnO solution and for sample A annealed at 170 °C for 4 h and at 210 °C for 0.5 and 1.5 h. The CIE coordinates confirm that as the temperature and the residence time increased, a change in the color, from blue to cyan, was observed as a consequence of broader emission.

The optical properties of samples B and C were also recorded, under the same annealing conditions of sample A; (Fig. 6b and Fig. 6c, respectively). Figure 8 shows the peak emission intensity as a function of the temperature, time, and silica concentrations of samples A, B, and C. The best performance was recorded with sample A, which contained the lowest silica concentration; however, when the silica increased, the few luminescent particles yielded a lower emission intensity. In sample B, an increase in the emission intensity of two times can be observed, compared to the as-synthesized ZnO NPs (*dashed blue line*), when annealing at 170 °C for 6 h, and 190 °C for 2 h. At different temperatures, the same tendency is observed; in samples A and B there is a maximal point, then a decline in peak intensity, but in sample C at 150, 170, and 190 °C no inflection point is reached for the maximal time, due to the protection of the silica matrix; however, at 210 °C there is a rapid decrease in emission intensity.

Table 3 shows the emission intensity ratios of the powder composites of samples A, B, and C, compared to the bare ZnO NPs. As can be seen, sample A treated at 170 °C for 4 h showed an emission 2.6 times greater than that of the ZnO colloidal solution. The CIE coordinates confirm a color shift from blue to cyan as consequence of annealing conditions; this is more evident in sample A than in sample C.

Table 3 Properties of the ZnO@SiO₂ composites

	Emission ratio sample/ZnO bare		CIE coordinates	
	170 °C	210 °C	170 °C	210 °C
A	1.96 ⁱ	2.29 ^{iv}	$x = 0.156, y = 0.138^i$	$x = 0.161, y = 0.157^{iv}$
	2.66 ⁱⁱ	1.89 ^v	$x = 0.157, y = 0.142^{ii}$	$x = 0.169, y = 0.196^v$
	2.45 ⁱⁱⁱ	0.99 ^{vi}	$x = 0.159, y = 0.150^{iii}$	$x = 0.172, y = 0.211^{vi}$
B	1.65 ⁱ	1.82 ^{iv}	$x = 0.156, y = 0.139^i$	$x = 0.161, y = 0.159^{iv}$
	1.96 ⁱⁱ	1.74 ^v	$x = 0.157, y = 0.144^{ii}$	$x = 0.161, y = 0.165^v$
	2.04 ⁱⁱⁱ	1.48 ^{vi}	$x = 0.157, y = 0.147^{iii}$	$x = 0.163, y = 0.169^{vi}$
C	0.91 ⁱ	1.70 ^{iv}	$x = 0.157, y = 0.149^i$	$x = 0.157, y = 0.137^{iv}$
	0.96 ⁱⁱ	1.43 ^v	$x = 0.158, y = 0.153^{ii}$	$x = 0.158, y = 0.149^v$
	1.1 ⁱⁱⁱ	1.2 ^{vi}	$x = 0.158, y = 0.155^{iii}$	$x = 0.159, y = 0.150^{vi}$

i = 2 h, ii = 4 h, iii = 6 h, iv = 0.5 h, v = 1 h, vi = 1.5 h

4 Conclusions

ZnO nanoparticles were successfully confined in a silica matrix. The composites exhibited highly stability in water and enhanced blue emission centered at 440 nm. The photoluminescent properties of the composite were influenced by the silica concentration and the annealing treatment conditions. As the silica concentration increased from 80 to 90 mol%, the emission decreased, which was related to the small amount of fluorescent ZnO particles. However, a high percentage of silica prevented red shift emission caused by particle growth and agglomeration; as expected, maximal red shift was observed with sample A, heat treated at 210 °C for 1.5 h, but it was no greater than 20 nm. In TEM images and photoluminescence excitation spectra, higher crystallinity and a greater particle diameter were observed in the sample with a ratio of 20:80 annealed at 210 °C (10–13 nm), in comparison to the same sample treated at 170 °C (7–10 nm). Finally, the emission intensity of the 20:80 sample was enhanced 2.6 times when annealed at 170 °C for 4 h; this enhancement was attributed to the maximal solvent evaporation that occurs at 180 °C, as showed by TGA. Based on the bright and stable blue emission without red shift of the ZnO@SiO₂ composites, it is suggested their use in optoelectronic devices such as LEDs.

Acknowledgements The authors gratefully acknowledge the financial support of this work by the SIP-IPN projects 20170655 and 20170656 and by CNMN-IPN experimental support. Joan Reyes Miranda acknowledges the Conacyt PhD scholarship. The authors also would like to thank Henry Jankiewicz for the editing work that he did for this paper and M. García Murillo for her assistance.

Conflict of interest The authors declare that they have no competing interests.

References

- Yang Y, Zhao T, Cheng T, Shen J, Liu X, Yu B, Lv S, Zhang H (2014) Hepatotoxicity induced by ZnO quantum dots in mice. *RSC Adv* 4(11):5642–5648
- Ma Y, Chen M, Li M (2015) Hydrothermal synthesis of hydrophilic NaYF₄: Yb, Er nanoparticles with bright upconversion luminescence as biological label. *Materials Letters* 139:22–25
- Oliva J, Diaz-Torres L, Torres-Castro A, Salas P, Perez-Mayen L, De la Rosa E (2015) Effect of TEA on the blue emission of ZnO quantum dots with high quantum yield. *Optical Materials Express* 5(5):1109–1121
- Lin Y, Zhang Y, Zhao J, Gu P, Bi K, Zhang Q, Chu H, Zhang T, Cui T, Wang Y, Zhao J, Yu WW (2014) White-light-emitting diodes using GaN-excited CdSe/CdS/ZnS quantum dots. *Particology* 15:90–93
- Jacobsson TJ, Edvinsson T (2012) Antireflective coatings of ZnO quantum dots and their photocatalytic activity. *RSC Adv* 2(27):10298–10305
- Ding D, Lan W, Yang Z, Zhao X, Chen Y, Wang J, Zhang X, Zhang Y, Su Q, Xie E (2016) A simple method for preparing ZnO foam/carbon quantum dots nanocomposite and their photocatalytic applications. *Mater Sci Semicond Process* 47:25–31
- Pang A, Chen C, Chen L, Liu W, Wei M (2012) Flexible dye-sensitized ZnO quantum dots solar cells. *RSC Adv* 2(25):9565–9570
- Lin Y, Lin Y, Wu J, Tu Y, Zhang X, Fang B (2015) Improved performance of quantum dots sensitized solar cells using ZnO hierarchical spheres as photoanodes. *Ceram Int* 41 (10, Part B):14501–14507
- Brus LE (1984) Electron–electron and electron-hole interactions in small semiconductor crystallites: The size dependence of the lowest excited electronic state. *J Chem Phys* 80(9):4403–4409
- Zhang L, Yin L, Wang C, lun N, Qi Y, Xiang D (2010) Origin of Visible Photoluminescence of ZnO Quantum Dots: Defect-Dependent and Size-Dependent. *J Phys Chem C* 114(21):9651–9658
- Asok A, Gandhi MN, Kulkarni AR (2012) Enhanced visible photoluminescence in ZnO quantum dots by promotion of oxygen vacancy formation. *Nanoscale* 4(16):4943–4946
- Spanhel L, Anderson MA (1991) Semiconductor clusters in the sol-gel process: quantized aggregation, gelation, and crystal growth in concentrated zinc oxide colloids. *J Am Chem Soc* 113(8):2826–2833
- Wang X, Zhou S, Wu L (2013) Facile encapsulation of SiO₂ on ZnO quantum dots and its application in waterborne UV-shielding polymer coatings. *J Mater Chem C* 1(45):7547–7553
- Hagura N, Ogi T, Shirahama T, Iskandar F, Okuyama K (2011) Highly luminescent silica-coated ZnO nanoparticles dispersed in an aqueous medium. *J Lumin* 131(5):921–925
- Xu X, Xu C, Wang X, Lin Y, Dai J, Hu J (2013) Control mechanism behind broad fluorescence from violet to orange in ZnO quantum dots. *Cryst Eng Comm* 15(5):977–981
- Arslan O, Belkoura L, Mathur S (2015) Swift synthesis, functionalization and phase-transfer studies of ultrastable, visible light emitting oleate@ZnO quantum dots. *J Mater Chem C* 3(45):11965–11973
- Liu X, Xing X, Li Y, Chen N, Djerdj I, Wang Y (2015) Controllable synthesis and change of emission color from green to orange of ZnO quantum dots using different solvents. *New J Chem* 39(4):2881–2888
- Musat V, Tabacaru A, Vasile BS, Surdu V-A (2014) Size-dependent photoluminescence of zinc oxide quantum dots through organosilane functionalization. *RSC Adv* 4(108):63128–63136
- Dong H, Chen YC, Feldmann C (2015) Polyol synthesis of nanoparticles: status and options regarding metals, oxides,

- chalcogenides, and non-metal elements. *Green Chem* 17 (8):4107–4132
20. Matsuyama K, Ihsan N, Irie K, Mishima K, Okuyama T, Muto H (2013) Bioimaging application of highly luminescent silica-coated ZnO-nanoparticle quantum dots with biotin. *J Colloid Interface Sci* 399:19–25
 21. Bouropoulos N, Tsiaoussis I, Pouloupoulos P, Roditis P, Baskoutas S (2008) ZnO controllable sized quantum dots produced by polyol method: An experimental and theoretical study. *Mater Lett* 62 (20):3533–3535
 22. Mezni A, Kouki F, Romdhane S, Warot-Fonrose B, Joulié S, Mlayah A, Samia Smiri L (2012) Facile synthesis of ZnO nanocrystals in polyol. *Mater Lett* 86:153–156
 23. Panigrahi S, Bera A, Basak D (2009) Encapsulation of 2–3-nm-Sized ZnO Quantum Dots in a SiO₂ Matrix and Observation of Negative Photoconductivity. *ACS Appl Mater Interfaces* 1(10):2408–2411
 24. Neaime C, Amela-Cortes M, Grasset F, Zakhour M, Molard Y (2016) Preparation of colloidal solution of silica encapsulating cyanobiphenyl unit-capped ZnO QD emitting in the blue region. *Dalton Trans.*
 25. Panasiuk YV, Raevskaya OE, Stroyuk OL, Kuchmiy SY, Dzhang VM, Hietschold M, Zahn DRT (2014) Colloidal ZnO nanocrystals in dimethylsulfoxide: a new synthesis, optical, photo- and electroluminescent properties. *Nanotechnology* 25(7):075601
 26. Panigrahi S, Bera A, Basak D (2011) Ordered dispersion of ZnO quantum dots in SiO₂ matrix and its strong emission properties. *J Colloid Interface Sci* 353(1):30–38
 27. Reyes Miranda J, García Murillo A, de J, Carrillo Romo F, Oliva Uc J, Flores Sandoval CA, de J, Morales Ramírez A, Velumani S, de la Rosa Cruz E, Garibay Febles V (2014) Synthesis and optical properties of BaTiO₃:Eu₃₊@SiO₂ glass ceramic nano particles. *Journal of Sol-Gel Science and Technology* 72(3):435–442
 28. Klein LC (1985) Sol-Gel Processing of Silicates. *Ann Rev Mater Sci* 15(1):227–248
 29. Socrates G (2001) Infrared and Raman Characteristics Group Frequencies. Tables and Charts. John Wiley & Sons, England
 30. Harder P, Grunze M, Dahint R, Whitesides GM, Laibinis PE (1998) Molecular Conformation in Oligo(ethylene glycol)-Terminated Self-Assembled Monolayers on Gold and Silver Surfaces Determines Their Ability To Resist Protein Adsorption. *The Journal of Physical Chemistry B* 102(2):426–436
 31. Nanda M, Yuan Z, Qin W, Poirier M, Chunbao X (2014) Purification of Crude Glycerol using Acidification: Effects of Acid Types and Product Characterization. *Austin J Chem Eng* 1(1):1004
 32. Tang X, Choo ESG, Li L, Ding J, Xue J (2009) One-Pot Synthesis of Water-Stable ZnO Nanoparticles via a Polyol Hydrolysis Route and Their Cell Labeling Applications. *Langmuir* 25(9):5271–5275
 33. Catauro M, Dell’Era A, Vecchio Cipriotti S (2016) Synthesis, structural, spectroscopic and thermoanalytical study of sol-gel derived SiO₂-CaO-P₂O₅ gel and ceramic materials. *Thermochim Acta* 625:20–27
 34. Ravaine D, Seminel A, Charbouillot Y, Vincens M (1986) A new family of organically modified silicates prepared from gels. *Journal of Non-Crystalline Solids* 82(1–3):210–219
 35. Ștefănescu M, Stoia M, Ștefănescu O, Popa A, Simon M, Ionescu C (2007) The interaction between TEOS and some polyols. *Journal of Thermal Analysis and Calorimetry* 88(1):19–26
 36. Huang JJ, Ye YB, Lei ZQ, Ye XJ, Rong MZ, Zhang MQ (2014) Highly luminescent and transparent ZnO quantum dots-epoxy composite used for white light emitting diodes. *Phys Chem Chem Phys* 16(12):5480–5484
 37. Raevskaya AE, Panasiuk YV, Stroyuk OL, Kuchmiy SY, Dzhang VM, Milekhin AG, Yeryukov NA, Sveshnikova LA, Rodyakina EE, Plyusnin VF, Zahn DRT (2014) Spectral and luminescent properties of ZnO-SiO₂ core-shell nanoparticles with size-selected ZnO cores. *RSC Adv* 4(108):63393–63401
 38. Kumar V, Kumar V, Som S, Yousif A, Singh N, Ntwaeaborwa OM, Kapoor A, Swart HC (2014) Effect of annealing on the structural, morphological and photoluminescence properties of ZnO thin films prepared by spin coating. *J Colloid Interface Sci* 428:8–15